Nuclear Instruments and Methods in Physics Research A245 (1986) 351–360
North-Holland, Amsterdam

RADIATION ON F2 LEAD GLASS AND CONSEQUENCES FOR THE MONITORING OF THE ABSOLUTE CALIBRATION OF LEAD GLASS CALORIMETERS

Kim KIRSEBOM

Institute of Physics, University of Oslo, N-0316 Oslo 3, Norway

Roger SOLLIE

Institute of Theoretical Physics, University of Trondheim, N-7034 Trondheim-NTH, Norway

Received 15 November 1985

The effect of radiation on the transmission properties of F2 lead glass has been investigated for wavelengths $350 \leqq \lambda \leqq 700$ nm and absorbed doses $0 \leqq D \leqq 5000$ rad. We parametrize the effect as $a(\lambda, D) = 1 - \exp(-\mu_R(\lambda)D)$ and determine $\mu_R(\lambda)$ both when the radiation environment is that of a hadron collider (ISR at CERN) and that of a ^{60}Co source (purely electromagnetic radiation). The resultant effect, taking into account emission spectrum, transmission and quantum efficiencies, is calculated for a specific experimental setup. The effect clearly (and unfortunately) is quite dependent on x, the distance the light has to cover in lead glass before detection. We also propose how the absorbed dose could be monitored by means of two monitoring systems. This is intimately related to the task of finding the time dependence of the absolute calibration which is the topic of the last section.

1. Introduction / what has been measured

We used F2 * lead glass (LG) as absorber material for our electromagnetic calorimeters in the R704 ISR experiment [1]. These detectors and their role in the experiment are briefly presented below (see sect. 4). One major requirement for the calorimeters naturally was that they should maintain a good and adequate energy resolution throughout the periods of data taking. We therefore were very concerned about a possible "yellowing" of the LG. This effect is caused by the absorption of radiation and leads to a reduced photon transmission efficiency at shorter photon wavelengths, hence the term yellowing.

The radiation induced reduction in the transmission efficiency will be referred to as "radiational absorption", RA. It is a function of two variables, λ, the wavelength and, D, the absorbed dose ** and will be denoted as $a(\lambda, D)$. a is, to be explicit, defined as the dose-dependent relative increase in the loss of photons at a certain wavelength and through 1 cm of LG:

$$a(\lambda, D) \equiv 1 - \frac{T(\lambda, D, x = 1)}{T(\lambda, D = 0, x = 1)}, \tag{1}$$

where T is the transmission efficiency (or simply the number of transmitted photons), and x is the LG thickness (in cm) traversed by the photons.

It should be noted that coping with an appreciable amount of yellowing is far from trivial in calorimetry; this requires knowing the correction factor which when multiplied to the recorded signals will make up for the lost light. To find this factor one would need both (a), a monitoring system allowing the disentangling and measuring of the transmission efficiency alone (with a single photomultiplier per LG block, which was our case, one only sees fluctuations in the overall gain comprising fluctuations in the transmission and photocatode conversion efficiencies and in the photomultiplier gain) and (b), full knowledge of the geometry of all electron and positron tracks in every electromagnetic shower which is to be used for energy measurements.

For the purpose of measuring in a controlled and independent way the RA as a function of both the photon wavelength, λ, and the absorbed dose, D, we had made special LG prisms 2 and 4 cm thick. These were then exposed to typical ISR radiation throughout 4 exposure periods in 1983. The absorbed doses were monitored with three types of dosimeters, RPL-glass (radiophotoluminescence glass) LiF6 and LiF7 and after

* Produced by Glaswerk Schott/Mainz/FRG. Characteristic data: 1 rad length = 3.05 cm, critical energy = 18.2 MeV, density = 3.61 g/cm^3, ref. index (at $\lambda = 480$ nm) = 1.633, ser. prod. number: 620364.

** In this paper doses are given in the somewhat oldfashioned unit of rad. 1 rad = 0.01 Gy = 0.01 J/kg.

each exposure the RAs of the LG prisms were measured. In total we had 8 prisms which were irradiated in the ISR tunnel. Also separate prisms were exposed to ^{60}Co radioactive sources; the doses being 10, 100 and 1000 rad when measured with RPL dosimeters. This radiation is purely electromagnetic (γ's of 1.17 and 1.33 MeV).

The comparison between a_{ISR} and $a_{^{60}Co}$ will show how damaging to the transmission properties of LG the absorption of the same dose (measured again with RPL-meters) in two different radiation environments is; that of a hadron–hadron collider (the ISR) and that of only electromagnetic components (^{60}Co). However, since our main concern was understanding the effect of the ISR irradiation, we accumulated much more data exposing the prisms in the ISR than exposing them to ^{60}Co sources. Therefore note that, while the ISR data will elucidate the λ and D dependence of the RA, the ^{60}Co data will lead to values for the same quantity which presumably are more useful and relevant to the reader since in this case the source and composition of the radiation is fully known.

2. Data

The data are presented in tables 1 and 2, and figs. 1a–1d.

In table 1 we show all data concerning one of the prisms (labelled 2-1) irradiated in the ISR. For each of the 4 exposures several values of the absorbed doses are given, and $a(\lambda, D)$ is tabulated at 6 wavelengths. Equivalent information exists for the 7 other prisms. Three types of dosimeters were used: RPL-dosimeters, which is a glass type dosimeter sensitive to all kinds of radiation except fast neutrons (i.e. gammas, charged particles and thermal neutrons), TLD LiF6 dosimeters, sensitive to neutrons and gammas and lastly TLD LiF7 dosimeters which only measure gamma radiation. For the RPLs three dose values are given. "Single" is the dose throughout one period of exposure measured with a dedicated RPL dosimeter, "add." corresponds to the integrated dose starting 28.2.83 calculated by adding the "single" doses, and "acc." finally is also the integrated dose, but this time measured by one single dosimeter which was read after each exposure. Naturally "add." and "acc." should be the same. The disagreement says something about the precision in the dose measurements; for the purpose of both cross-checking these measurements and evaluating their precision, we had installed many dosimeters of all types before each exposure. Also presented in table 1 are the doses recorded by the LiF6 and LiF7 dosimeters. There are two entries per exposure and type of dosimeter: The left one represents the "single" dose and the right one the "added" dose. Many more details about the dose measurements

Table 2
^{60}Co irradiation on several prisms. As in table 1, the entries represent $a(\lambda, D)$ given in %.

Wavelength, λ (nm)	Dose (rad)		
	10	100	1000
350	0.631	1.20	7.85
400	0.344	0.964	6.51
450	0.246	0.719	4.76
500	0.143	0.553	3.12
600	0.057	0.338	1.38
700	≡ 0	0.250	0.963

Table 1
ISR irradiation on prism no. 2-1. In the top part of the table are given doses relating both to the exposure period in question and to the full exposure since the beginning (28.2.83); these doses were measured with various dosimeters, see text. In the lower part is presented the RA in %. $a(\lambda, D)$ was measured after each exposure.

Dose, D (rad)	Exposure no.1 28.2 → 25.3	Exposure no. 2 6.4 → 9.5	Exposure no. 3 16.5 → 7.7	Exposure no. 4 15.8 → 16.12
RPL Single	28	243	448	2200
RPL Add.	28	271	719	2919
RPL Acc.	–	–	711	2668
LiF7	21	154 175	352 527	2880 3407
LiF6	200	96 296	448 744	159 903
Wavelength, λ (nm)	Radiational absorption, $a(\lambda, D)$ in %			
350	–	–	–	9.86
400	0.137	1.58	2.36	7.72
450	0.105	1.19	1.67	5.23
500	0.082	0.78	1.11	3.27
600	0.082	0.42	0.53	1.21
700	0.082	0.26	0.42	0.81

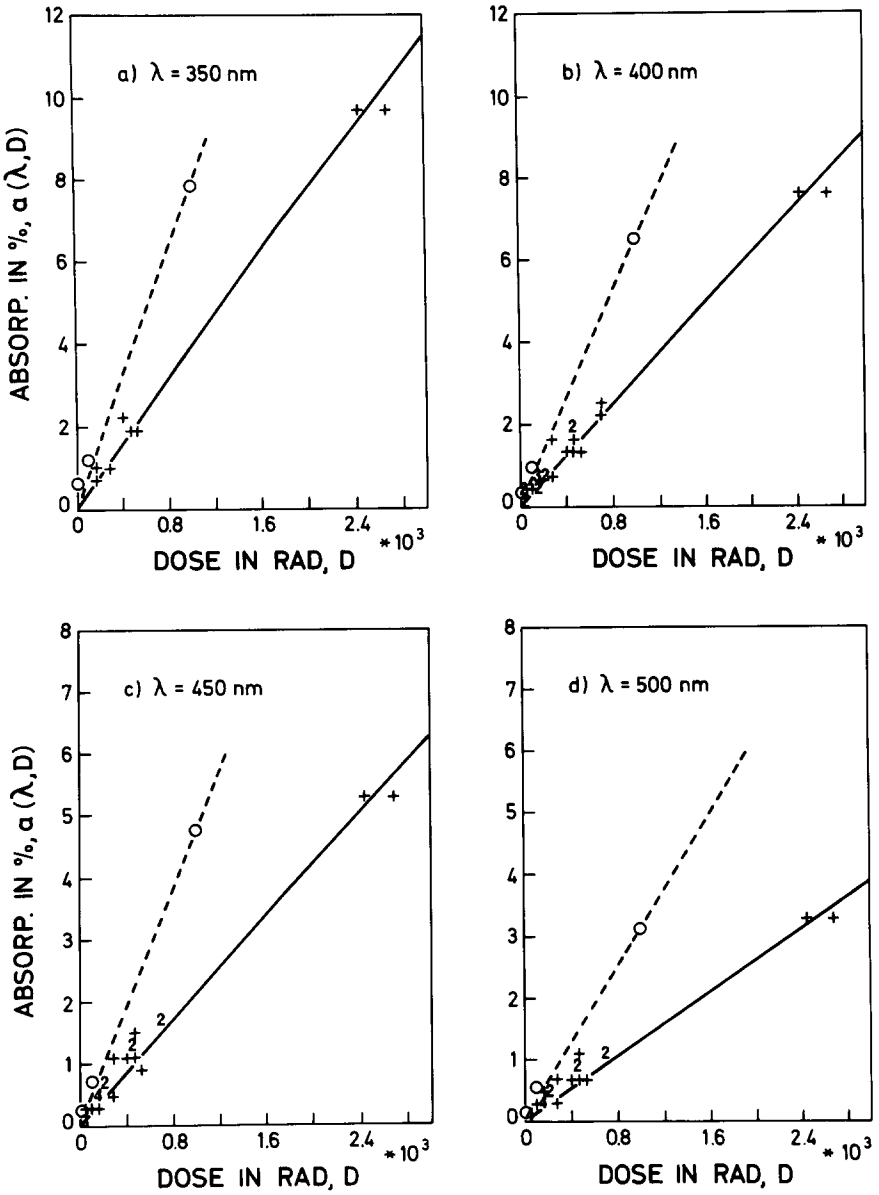

Fig. 1. The radiational absorption $a(\lambda, D)$ as a function of the absorbed dose D for (a) $\lambda = 350$ nm, (b) $\lambda = 400$ nm, (c) $\lambda = 450$ nm, and (d) $\lambda = 500$ nm. These results correspond to direct measurements on 2 and 4 cm thick prisms. Data points denoted +, 2, 3 etc. refer to samples having been exposed in the ISR, while those denoted with circles (○) refer to samples being exposed to ^{60}Co irradiation. The curves are fits of $a(\lambda, D) = 1 - \exp(-\mu_R D)$ to the data points. Doses were measured with RPL dosimeters.

and the calculations/normalizations involved in determining $a(\lambda, D)$ are to be found in ref. [2].

The results of several controlled irradiations carried out by experts from the Radiation Protection Group at CERN are presented in table 2. Again what is tabulated is $a(\lambda, D)$ in percent. The values for D were chosen so as to extract as much information as possible; mostly guessing, but also following suggestions from other "LG physicists". The data in table 2 involve several prisms.

Finally all the data at 4 wavelengths, both concerning ISR and ^{60}Co irradiations, are presented in the scatterplots of figs. 1a–1d; "+", "2" etc. represent one, two etc. entries from the sample of exposures having taken place in the ISR, and circels "0" come from the data obtained with the ^{60}Co radioactive sources. The curves are fits to the data and will be explained below.

3. Discussion of the data

A nice nearly linear correlation is seen to exist between the absorbed dose and the RA. In this case the added RPL dose has been used along the abscissa. Also the added LiF7 dose could have been used. This would have led to a slightly worse correlation (the belt of correlation would have broadened). Lastly, employing the added LiF6 dose would not make much sense; showing a very weak and nonlinear correlation with the RA, this type of dosimeter is clearly rather insensitive to the type of radiation which degrades the transparency of LG. Concerning the width of the belt of correlation when using RPL as dose monitors (see fig. 1) this could to a very large extent be attributed to the rather poor precision of the dose measurements. $\sigma_{D,rel}$ typically $\cong 10\%$ for $D > 1000$ rad, $\sigma_{D,rel} > 10\%$ for $D < 1000$ rad and for $D < 100$ rad, $\sigma_{D,rel}$ may attain 50%! On the other hand $\sigma_{a,rel}$ could be controlled to the level of some percent (1–3%).

$a(\lambda, D)$ was parametrized as $1 - \exp(-\mu_R D)$ where $\mu_R = \mu_R(\lambda)$ is the radiation absorption coefficient. The curves in figs. 1a–1d represent fits of this function to the data. Notice that there are two fits at each wavelength, one for the ISR data, another for the data of the ^{60}Co exposures. The resulting λ-dependence of μ_R is shown in fig. 3 and table 3.

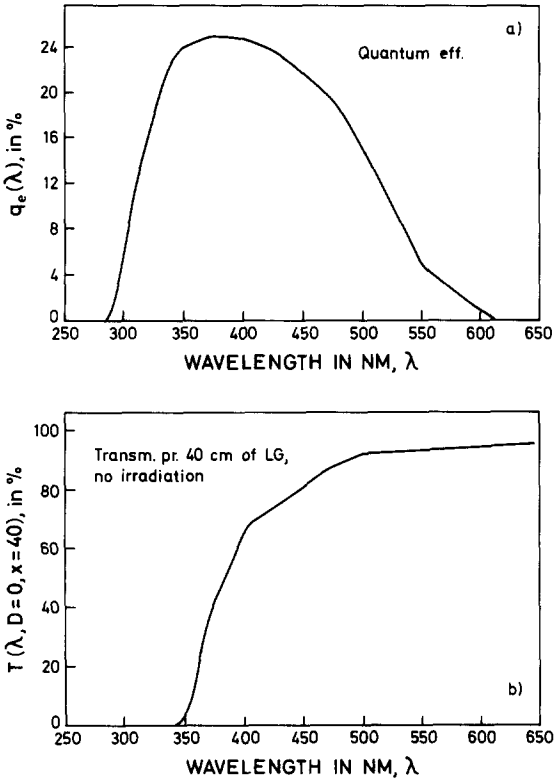

Fig. 2. (a) Typical quantum efficiency for our PMs (EMI 9928 KA with bialkalie cathodes). (b) Transmission efficiency for 40 cm nonirradiated F2 LG.

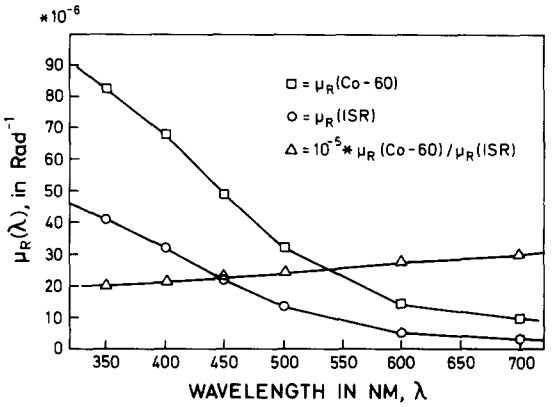

Fig. 3. The λ-dependence of the radiation absorption coefficient. The vertical scale when taken without dimension is correct also for the curve of 10^{-5} times the μ_R-ratio.

Table 3
The radiation absorption coefficient

Wavelength, λ (nm)	$\mu_R(^{60}\text{Co})$ (rad^{-1})	$\mu_R(\text{ISR})$ (rad^{-1})	$\frac{\mu_R(^{60}\text{Co})}{\mu_R(\text{ISR})}$
350	0.823×10^{-4}	0.407×10^{-4}	2.02
400	0.677×10^{-4}	0.318×10^{-4}	2.13
450	0.490×10^{-4}	0.216×10^{-4}	2.27
500	0.320×10^{-4}	0.133×10^{-4}	2.41
600	0.141×10^{-4}	0.509×10^{-5}	2.77
700	0.968×10^{-5}	0.324×10^{-5}	2.99

Notice that the parametrization of $a(\lambda, D)$ is natural. Choose a very small dose d, the relative * transmission becomes $t = 1 - \delta_a$ where δ_a represents a very small absorption, $\delta_a \ll 1$. The effect of the dose d is to reduce the "detectable fraction of light" from 1 to $1 - \delta_a$; applying the same dose a second time the detectable fraction would drop to $(1 - \delta_a)^2$. Therefore a non-infinitesimal dose D will lead to the relative transmission: $t(D) = (1 - \delta_a)^{D/d} = e^{-\delta_a D/d} = e^{-\mu_R D}$ where $\mu_R = \delta_a/d = -\mathrm{d}t/\mathrm{d}D \mid_{D=0}$.

In fig. 3 is also shown the ratio $\mu_R(^{60}\text{Co})/\mu_R(\text{ISR})$. This ratio varies slowly with λ, within $\pm 20\%$ for $350 \leqq \lambda \leqq 700$ nm. Hence, apart from a scaling parameter in μ_R, the behaviour of $a(\lambda, D)$ does not depend on the type of radiation. For small doses it is seen that $a_{^{60}\text{Co}}/a_{\text{ISR}} = \mu_R(^{60}\text{Co})/\mu_R(\text{ISR})$. Actually, in the worst case, for $\lambda = 350$ nm and $D = 2500$ rad, this approxi-

* The relative transmission is defined as $T(D)/T(D = 0)$.

mation is correct to within 5%. Fig. 3 therefore shows that the radiation of ^{60}Co leads to an RA 2–3 times above that produced by the radiation in the ISR. In other words, ^{60}Co is seen to be 2–3 times as damaging to F2 LG as a hadron collider.

4. The electromagnetic calorimeters in R704

We used sandwich lead/scintillator calorimeters $4.7X_0$ (= radiation lengths) deep in conjunction with our LG calorimeters for the detection and energy measurement of photons, electrons and positrons produced in decays of various charmonium states. For example, the χ_2 state was studied through the electromagnetic transitions $\chi_2 \to \gamma\psi \to \gamma\, e^+\, e^-$.

There were two identical LG calorimeters, one per arm, each being composed of 66 individual blocks of dimension 15×15 cm^2 (facing the vertex) and 30 cm deep ($= 10X_0$), all sides rectangular. A 13 cm diameter photomultiplier which would collect a large fraction of the Cherenkov light produced by an electromagnetic shower was glued onto the 15×15 cm^2 side facing away from the vertex. The maximum electromagnetic energy which could be deposited in a single LG block was roughly 5 GeV.

5. What would be the actual effect on the photomultiplier (PM) output signals of a certain RA?

Now, having measured $a(\lambda, D)$, we *calculate* the expected "reduced" PM output signal, i.e.

$$S(D, x) \equiv \frac{q(D, x)}{q(D=0, x)}, \tag{2}$$

where q is the average PM output signal produced by a point-like light source whose photons traverse x cm of LG before impinging on the cathode, and D is the dose. q is calculated taking into acccount the emission spectrum of the source $d(\lambda)$, the overall transmission efficiency $T(\lambda, D, x)$ in LG, the photocathode quantum efficiency $q_e(\lambda)$, a geometrical acceptance $A(x)$ **, and finally the gain of the dynode chain, M. Therefore,

$$q(D, x) = M\, A(x) \int_{\lambda_{low}}^{\lambda_{high}} d(\lambda) T(\lambda, D, x) q_e(\lambda)\, d\lambda. \tag{3}$$

Here λ_{low} and λ_{high} are lower and higher limits for the q_e-distribution; $q_e(\lambda) = 0$ for $\lambda \leqq \lambda_{low} = 290$ nm and

** $A(x)$ includes (1), the probability that the photon be emitted so that the length of its trajectory to the cathode becomes x, and (2) all the nonabsorption inefficiencies such as imperfect reflecting on sidewalls and wrapping of the LG-block and also the actual escape of photons from the block.

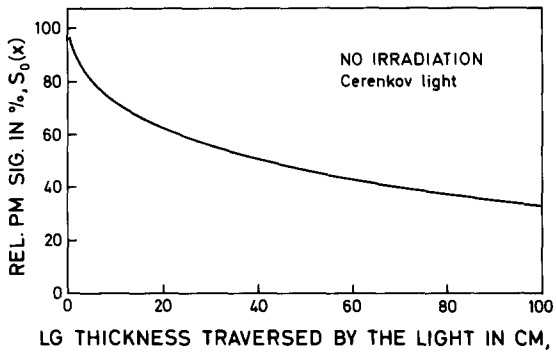

Fig. 4. The effect of absorption in nonirradiated LG on Cherenkov photons, $S_0(x) = q(D=0, x)/q(D=0, x=0)$ where $q(D, x)$ is defined by eq. (3).

$\lambda \geqq \lambda_{high} = 620$ nm. $q_e(\lambda)$ is shown in fig. 2a and represents the typical quantum efficiency of our PMs †. From eq. (1) we find,

$$T(\lambda, D, x=1) = T(\lambda, D=0, x=1)\,(1 - a(\lambda, D)) \equiv T_0(\lambda)(1 - a(\lambda, D)). \tag{4}$$

Furthermore the x-dependence is given by

$$T(\lambda, D, x) = [T(\lambda, D, x=1)]^x. \tag{5}$$

This relation has been checked experimentally using 2, 5, 10, 20 and 40 mm thick prisms (see again ref. [2]). The result not only confirmed the validity of eq. (5), but what is more important, showed us that we knew how to handle the light reflections which were involved in making all the transmission and absorption measurements referred to in this paper.

Inserting eqs. (4) and (5) in eq. (3) one gets,

$$q(D, x) = M\, A(x) \int_{\lambda_{low}}^{\lambda_{high}} d(\lambda) \times [T_0(\lambda)(1 - a(\lambda, D))]^x q_e(\lambda)\, d\lambda, \tag{6}$$

Now we want to calculate the *integral* of eq. (6). $d(\lambda)$, the emission spectrum of the source, is to be varied. $T_0(\lambda)$ is known; this quantity was measured several times by us (carrying out the RA measurements one needs a nonirradiated reference prism) and was also provided by the manufacturer. $T(\lambda, D=0, x=40) = (T_0(\lambda))^{40}$, is shown in fig. 2b. The parametrization of $a(\lambda, D)$ was explained above in sect. 3 and finally for $q_e(\lambda)$ we used data supplied by EMI (see fig. 2a). Inserting for $d(\lambda)$ and calculating the integral numerically, several interesting quantities may be determined for our experimental setup:

(1) Let $d(\lambda) = \text{constant}/\lambda^2$, i.e. the photons are distributed as Cherenkov photons (= "physics" photons). Then in fig. 4 is shown the effect of absorption in

† Type EMI 9928 KA, $\phi = 12.5$ cm, bialkali cathode (CsK_2Sb) and 11-stage venetian blind dynode structure.

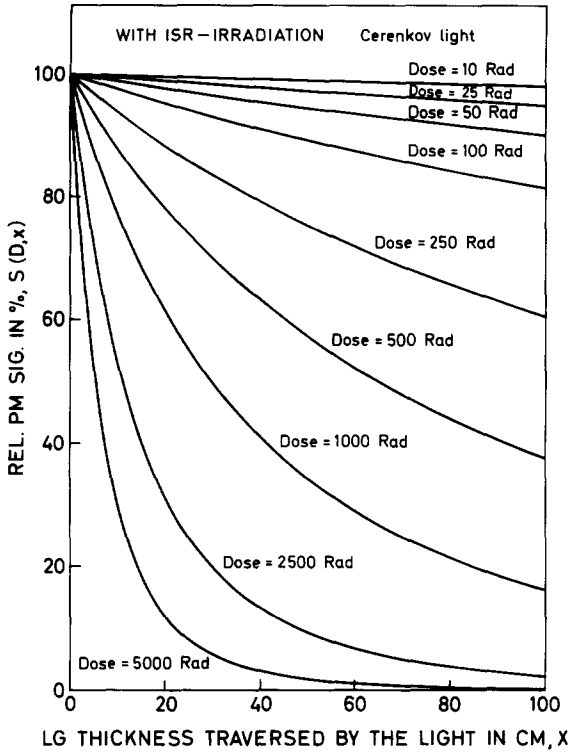

Fig. 5. The effect of yellowing on Cherenkov photons for various doses; $S(D, x) = q(D, x)/q(D = 0, x)$. The LG is exposed to the radiation of a hadron collider.

absence of any irradiation:

$$S_0(x) \equiv q(D = 0, x)/q(D = 0, x = 0).$$

It is seen that at $x = 43$ cm we are left with half the signal we would have at $x = 0$ cm.

(2) Again let $d(\lambda) = \text{constant}/\lambda^2$. Furthermore let $a(\lambda, D) = a_{\text{ISR}}(\lambda, D)$ which means that the LG is exposed to typical radiation of a hadron collider. The measurable effect of yellowing is given by

$$S(D, x) = q(D, x)/q(D = 0, x).$$

$S(D, x)$ is found (a) in fig. 5 as a function of x for various values of D, and (b) in fig. 6a as a function of D for various values of x. Notice that this is the yellowing effect when all the Cherenkov photons have been generated at a *fixed* distance x from the photocathode. Naturally this is far from real life; integrating over x will be discussed in the following section. From figs. 5 and 6a it is seen that with doses of 100, 250, 500, 1000, 2500 and 5000 rad we would observe a reduced signal, $S = 0.9$ (corresponding to a 10% loss) if the light originated respectively at distances of 45.0, 17.3, 7.8, 3.8, 1.47 and 0.74 cm from the photocathode.

(3) We still consider Cherenkov light, but this time $a(\lambda, D) = a_{^{60}\text{Co}}(\lambda, D)$. Again we assume exposure do-

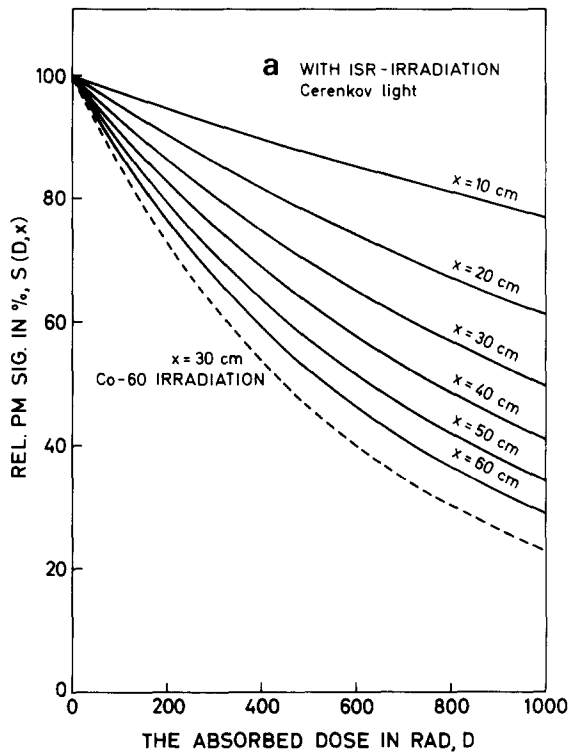

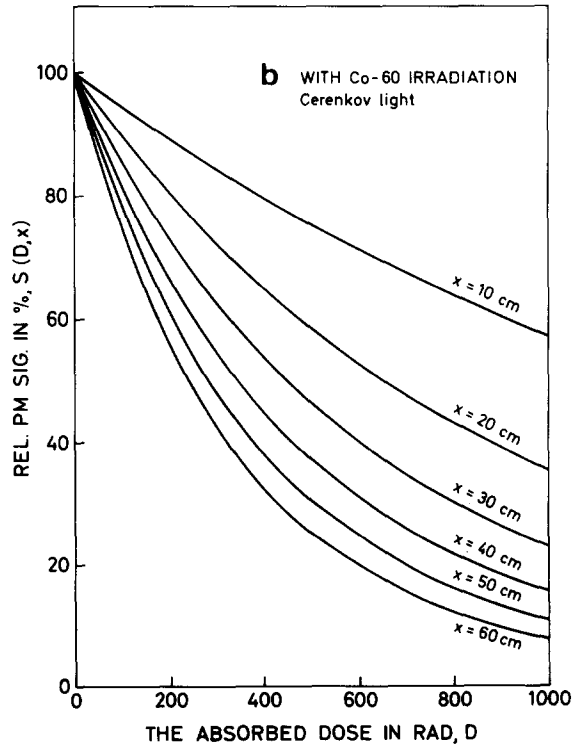

Fig. 6. (a) Same as fig. 5, but for various x. Notice the dashed curve, shown here to help compare the effects of the two types of radiation. (b) Same as (a), but the LG is here exposed to purely electromagnetic radiation from ^{60}Co.

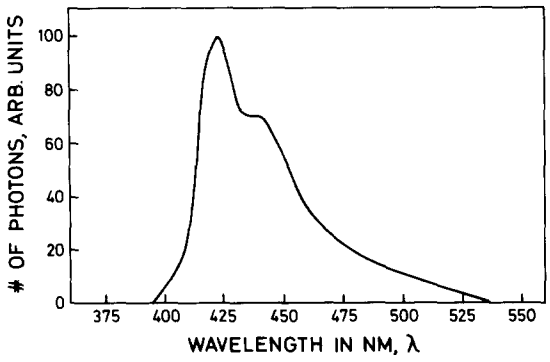

Fig. 7. The emission spectrum of the NE102A scintillator.

ses of 100, 250, 500, 1000, 2500 and 5000 rad and require a 10% RA. In this case the light would have to originate respectively at distances of only 19.0, 7.6, 3.53, 1,73, 0.69 and 0.38 cm from the photocathode (see fig. 6b). Thus the factor 2–3 effect discussed above in sect. 3 (^{60}Co versus ISR-radiation) also applies when actual PM signals are considered. This is to be expected since $\mu_R(^{60}\text{Co})/\mu_R(\text{ISR})$ varies slowly with λ.

(4) $d(\lambda) \neq \text{constant}/\lambda^2$. This is relevant for light sources used for monitoring purposes. For example, if $d(\lambda)$ is the scintillation light spectrum of fig. 7, then in fig. 8 is shown $S(D,\ x = 30)$. The RA can be monitored by means of two such well known light sources. This in turn may allow to correct for the light lost due to yellowing. All of this will be explicated below.

6. One possible recipe for monitoring and controlling the absolute calibration of LG-counters which are exposed to radiation

Assume that the LG-counters are read with PMs. Two correction factors are needed. Let q be the charge of the PM output signal and t the time, then

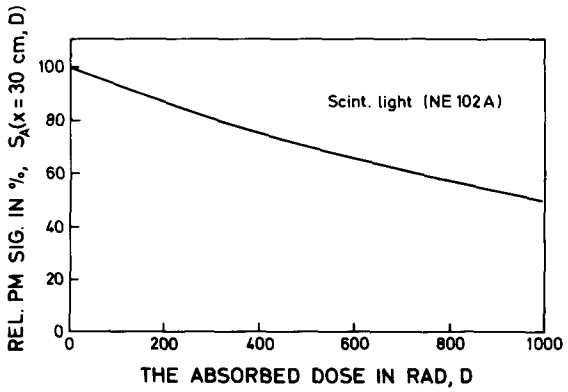

Fig. 8. The effect of yellowing on scintillation light emitted at a distance of 30 cm from the cathode.

$$q(t=0) = C_T(t)C_G(t)q(t), \tag{7}$$

where $C_T(t)$ corrects for changes in the LG transmission efficiency and C_G for variations in the gain (= PM quantum efficiency × PM-gain). Note that while C_G is source independent (does not depend on the wavelength), this is not at all true for C_T which does depend on the origin of the light.

In the R704 experiment mentioned above we did not perform a detailed monitoring which allowed to determine C_T and C_G separately; for two reasons: (1) the requirements on the energy resolution were not severe; and (2) the RA was believed to be modest.

However, we did have the hardware for performing such a monitoring. The system was based on two light sources with well separated emission spectra. One peaking at 422 nm, was that of scintillation light shown in fig. 7. This was produced by a radioactive ^{241}Am source emitting 5.5 MeV α-particles into a small tablet of NE102A scintillator which was glued onto the LG. The other was that of a monochromatic and yellow LED (light emitting diode) peaking at 580 nm. While the scintillation light travelled 30 cm in LG before reaching the photocathode (coming from the americium sources sitting on the upstream 15×15 cm^2 ends of the LG-blocks) the LED-light covered twice this distance. This light was fed into the LG-blocks via optical fibers connected close to the PMs on the downstream ends [3].

We also mention that a third monitoring system existed and was operational during the last 4 months of data-taking in 1984. This was based on a flashing argon lamp producing blue light ($\lambda_{max} = 425$ nm) which was transported into the LG-blocks in exactly the same way as the LED-light. Data from this system allowed us to conclude that throughout the 4 month period, the global radiational absorption on the 132 LG-blocks most likely did not exceed some percent [4].

In the following discussion on how one could determine $C_T(t)$ and $C_G(t)$, the blue light source might also have been the flashing argon lamp. For simplicity we shall only consider the americium scintillation light. When it comes to applications a choice between the two systems should be based on parameters such as reliability and precision.

As subscript, let L refer to quantities related to the LED-system, A to quantities of the americium system and C to quantities of Cherenkov photons. Also let 0 as a superscript denote the value at time zero, $t = 0$. We want to determine $C_T(t)$ and $C_G(t)$ when the following charges are known:

$$q_L(t),\ q_A(t),\ q_C(t),\ q_L(t=0) = q_L^0$$

and

$$q_A(t=0) = q_A^0.$$

If sufficient amount of information is available, theses changes *may* be calculated, for example,

$$q_A(t) = A_A(t)M(t)\int_{\lambda_{low}}^{\lambda_{high}} d_A(\lambda, t)T(\lambda, D, x_A, t) \times q_e(\lambda, t)\,d\lambda, \quad (8)$$

where $d_A(\lambda, t)$ is the emission spectrum for scintillation light at time t. We assume that $d_A(\lambda, t) = d_A(\lambda, t=0) \equiv d_A(\lambda)$. $T_A(\lambda, D, x_A, t)$ is the transmission efficiency at time t. It is natural to set $T_A(\lambda, D, x_A, t) = T_A(\lambda, D, x_A, t=0) \equiv T_A(\lambda, D, x_A)$ since the t-dependence only enters through the absorbed dose D. T is given by eqs. (4) and (5). x_A is the mean distance to the cathode; $x_A = 30$ cm. $q_e(\lambda, t)$ is the quantum efficiency. We shall assume that $C_q(t)q_e(\lambda, t) = q_e(\lambda, t=0) \equiv q_e(\lambda)$. $A_A(t)$ is the average geometrical acceptance. We set $A_A(t) = A_A^0 \equiv A_A$. This quantity is assumed to be independent of x. Since a large fraction of the photons go directly to the cathode (without reflecting on the sidewalls), we may replace a varying x with a fixed $x = x_A$. $M(t)$ is the gain of the PM dynode chain.

Introducing these assumptions in eq. (8) we find:

$$q_A(t) = A_A M(t) C_q^{-1}(t)\int_{\lambda_{low}}^{\lambda_{high}} d_A(\lambda)T(\lambda, D, x_A) \times q_e(\lambda)\,d\lambda \equiv A_A M(t) C_q^{-1}(t) g_A(D), \quad (9)$$

and

$$q_A^0 = A_A M^0 g_A(D=0),$$

where naturally $C_q(t=0) = 1$. Let

$$S_A(D) \equiv \frac{g_A(D)}{g_A(D=0)}.$$

This function has been fixed numerically and is shown in fig. 8. The ratio of the charges at time zero and t is,

$$\frac{q_A^0}{q_A(t)} = \frac{M^0 C_q(t)}{M(t)} S_A^{-1}(D). \quad (10)$$

Almost equivalently one finds

$$q_L(t) = A_L M(t) C_q^{-1}(t) C_L^{-1}(t) g_L(D) \quad (11)$$

and

$$\frac{q_L^0}{q_L(t)} = \frac{M^0 C_q(t) C_L(t)}{M(t)} S_L^{-1}(D), \quad (12)$$

where the additional term $C_L(t)$ is justified by the unstability of the LED source,

$$d_L(t) \neq d_L^0.$$

We set $d_L^0 = C_L(t) d_L(t)$.

Hardwarewise $C_L(t)$ was monitored with photodiodes (pd) which, due to their very high stability, did not require any monitoring:

$$C_L(t) = \frac{q_{pd}^0}{q_{pd}(t)}.$$

Eqs. (10) and (12) contain two unknowns, D and $(M^0/M(t))C_q(t) = C_G(t)$. Dividing (10) by (12) one isolates D,

$$\frac{S_L(D)}{S_A(D)} = C_L(t)\,\frac{q_A^0}{q_A(t)}\,\frac{q_L(t)}{q_L^0}.$$

The function on the left may be tabulated in advance. Knowing the value of $S_L(D)/S_A(D)$ – all the quantities on the right side are measured – D may be found numerically. $C_G(t)$ is then determined from relation (10),

$$C_G(t) = \frac{M^0}{M(t)} C_q(t) = \frac{q_A^0}{q_A(t)} S_A(D), \quad (13)$$

Finally we perform the calculation of $C_T(t)$. For this purpose we define

$$g_C(D, x) = \int_{\lambda_{low}}^{\lambda_{high}} (1/\lambda^2) q_e(\lambda) T(\lambda, D, x)\,d\lambda. \quad (14)$$

Then one Cherenkov photon at a path length x to the cathode, moving along a vector pointing directly or indirectly to somewhere on the cathode surface and at a time t, so that $D(t) = D$, will, on the average, produce the signal

$$\hat{q}_C(D, x) = kM(t)C_q^{-1}(t)g_C(D, x), \quad (15)$$

where k is a normalization constant, $d_C(\lambda) = k/\lambda^2$. To calculate the signal from an electromagnetic shower one would need the length distribution $l_C(x)$ of the "good" photons. This tells how many photons would travel how far before reaching the cathode in absence of any absorption. Finding $l_C(x)$ therefore requires, as was also invoked in the introduction, full knowledge of the geometry of the electromagnetic shower plus tracking of all the individual Cherenkov photons through a completely transparent medium. The tracking of a photon ends either when the photon is absorbed on the sidewalls or is captured on the cathode. When the angle of incidence is too big, the photon will exit from the LG-block thus being exposed to holes and imperfections in the wrapping (reflecting aluminium foil).

Knowing $l_C(x)$, the charge of a shower is simply found by integrating over x,

$$q_C(D) = \int_0^\infty l_C(x)\hat{q}(D, x)\,dx. \quad (16)$$

From eq. (7)

$$C_T(t) = C_G^{-1}(t)\frac{q_C^0}{q_C(t)} = C_G^{-1}(t)\frac{q_C(D=0)}{q_C(D)}. \quad (17)$$

Since both D and $C_G(t)$ are already known, $C_T(t)$ in principle is determined.

The crucial point naturally is finding $l_C(x)$. What $l_C(x)$ should be applied in the case of a shower depositing a charge q_s on the anode? On average, to a certain shower charge q_s, corresponds a length distribution

$l_{q_s}(x)$. This relation could be established by Monte Carlo simulation methods. However, due to longitudinal and transversal fluctuations in the shower development, applying the same $l_{q_s}(x)$ to all showers with equal charge q_s, in principle is not correct. The error introduced may be reduced by letting $l_{q_s}(x) \to l_{q_s}(x;\ x',\ y',\ \theta,\ \phi)$ that is, by also taking into account the angles and coordinates at the point of impact. This huge task will not be considered here.

Instead observe that for $x \gtrsim 20$ cm and for modest doses, $D \lesssim 500$ rad, $\hat{q}_C(D,\ x)$ which is proportional to $g_C(D,\ x)$ will, to a rather good approximation, be a linear function of x (see figs. 5 and 6). If $\hat{q}_C$ is linear and in addition $l_C(x)$ is symmetric with mean value x_C, then we may rewrite eq. (16):

$$q_C(D) = \hat{q}_C(D,\ x_C)\int_0^\infty l_C(x)\,\mathrm{d}x = \hat{q}_C(D,\ x_C)N_C,$$

where N_C is the number of "good" photons in the shower. Inserting this in eq. (17), using eqs. (14) and (15) we find,

$$C_T(t) = C_G^{-1}(t)\frac{\hat{q}_C(D=0,\ x_C)}{\hat{q}_C(D,\ x_C)}$$

$$= C_G^{-1}(t)\ S_C^{-1}(D,\ x_C), \qquad (18)$$

where S_C is completely the equivalent of S_A and S_L for Cherenkov photons. This relation shows that if the assumptions of linearity and symmetry hold, then it will suffice to determine the value of x_C for each event in order to calculate $C_T(t)$. The function $S_C(D,\ x_C)$ is shown in figs. 5 and 6 (as $S(D,\ x)$). Its inverse, $S_C^{-1}(D,\ x_C)$, is seen to be equal to the overall correction factor $C_T(t)\ C_G(t)$.

We have also in fig. 9 established the correlation between the absorption of Cherenkov (= physics) light defined as $1 - S_C(D,\ x_C)$ and the absorption of the americium produced scintillation light, $1 - S_A(D,\ x_A)$. x_C takes on the values 30, 40 and 50 cm, while x_A is fixed at 30 cm. On the dashed line, $1 - S_C(D,\ x_C) = 1 - S_A(D,\ x_A)$. The figure shows that at a dose of for example 500 rad, 29.7% "of the scintillation light" * will be lost, while the loss for Cherenkov light will be respectively 30.2, 37.0 and 42.8% for $x_C = 30$, 40 and 50 cm. Still assuming $D = 500$ rad, what will be the error in $C_T(t)$ if one simply disregards that $l_C(x) \neq l_A(x)$ and $d_C(\lambda) \neq d_A(\lambda)$, i.e. sets $S_C(D,\ x_C) = S_A(D,\ x_A)$ in eq. (18)? Define the error as:

$$\Delta C_T(t,\ x_C) \equiv S_C(D,\ x_C) \times \left[S_C^{-1}(D,\ x_C) - S_A^{-1}(D,\ x_A)\right]$$

$$= 1 - \frac{S_C(D,\ x_C)}{S_A(D,\ x_A)}.$$

* Actually "of the americium produced scintillation photons which reach the cathode and here in turn convert into photoelectrons when $D = 0$".

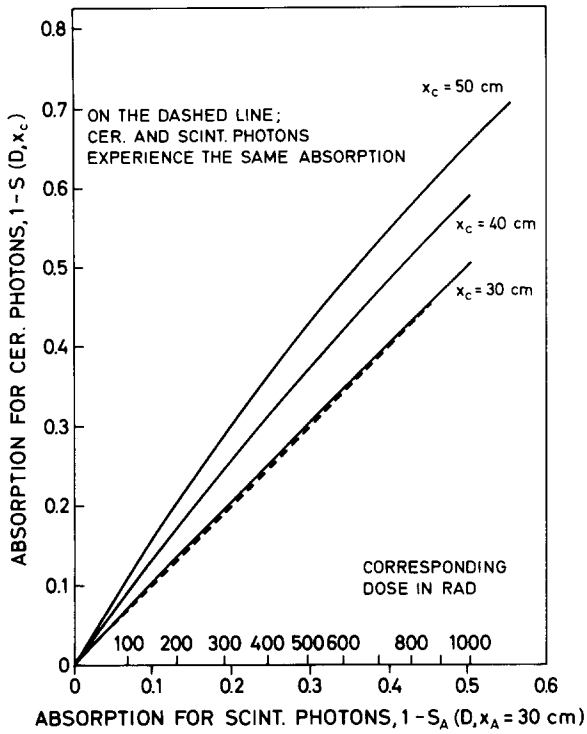

Fig. 9. The effect of yellowing as seen by Cherenkov photons vs scintillations photons. The former are generated at distances of 320, 40 and 50 cm from the cathode while the latter are emitted at a fixed distance of 30 cm. This correlation shows to what extent it is correct to monitor the yellowing (as seen by Cherenkov photons) with scintillation photons. See text for details.

Let x_A = constant = 30 cm, then $\Delta C_T(t,\ 30) = 0.7\%$, $\Delta C_T(t,\ 40) = 10.4\%$ and $\Delta C_T(t,\ 50) = 18.6\%$. Two conclusions may be drawn. First that some even very rudimentary knowledge of the length distribution $l_C(x)$ for the Cherenkov photons may greatly improve the determination of $C_T(t)$. Second that for $x_C = x_A = 30$ cm, and tacitly still assuming that $l_C(x)$ is symmetric, $\Delta C_T \equiv 0$. This is due to the fact that the scintillation spectrum is very similar to the Cherenkov spectrum when effects of attenuation and quantum efficiency have played their role and have "selected" the relevant parts in the spectra.

Acknowledgments

We wish to thank B. Baeyens, F. Coninckx, P. Maier, and H. Schönbacker of the CERN Radiation Protection Group who provided valuable assistance and facilities for carrying out the absorption and transmission measurements. We are also grateful towards Lars Leistam who as a CERN liaison physicist made possible the special preparation required for the LG prisms.

References

[1] C. Baglin et al., EP Internal Report 85-01 (January 18, 1985).
[2] R. Sollie, Internal R704 report, No. 62, CERN (September 1, 1983).
[3] B. Stugu, Thesis submitted at the Univesity of Oslo, Institute of Physics (May 27, 1983).
[4] L. Petrillo and M. Severi, Calibration Analysis, University of Rome (January 1985); Also as: Internal R704 report, No. 115.